European Journal of Cancer 109 (2019) 137–153

Available online at www.sciencedirect.com

ScienceDirect

journal homepage: www.ejcancer.com

Original Research

Sequence-dependent cross-resistance of combined radiotherapy plus $BRAF^{V600E}$ inhibition in melanoma

B. Shannan [a], J. Matschke [b], H. Chauvistré [a], F. Vogel [a], D. Klein [b], F. Meier [c], D. Westphal [c], J. Bruns [c], R. Rauschenberg [c], J. Utikal [d,e], A. Forschner [f], C. Berking [g], P. Terheyden [h], E. Dabrowski [i], R. Gutzmer [j], D. Rafei-Shamsabadi [k], F. Meiss [k], L. Heinzerling [l], L. Zimmer [a], Elisabeth Livingstone [a], Renáta Váraljai [a], A. Hoewner [a], S. Horn [a], J. Klode [a], M. Stuschke [m], B. Scheffler [a], A. Marchetto [n], G. Sannino [n], T.G.P. Grünewald [n,o,p], D. Schadendorf [a], V. Jendrossek [b], A. Roesch [a,*]

[a] *Department of Dermatology, University Hospital Essen, West German Cancer Center, University Duisburg-Essen and the German Cancer Consortium (DKTK) University of Duisburg-Essen, Germany*
[b] *Institute of Cell Biology (Cancer Research), University of Duisburg-Essen, Medical School, Germany*
[c] *Skin Cancer Center National Center for Tumor Diseases, Department of Dermatology, Medical Faculty and University Hospital Carl Gustav Carus, TU Dresden, Germany*
[d] *Skin Cancer Unit German Cancer Research Center (DKFZ), Heidelberg, Germany*
[e] *Department of Dermatology, Venereology and Allergology University Medical Center Mannheim, Heidelberg University, Mannheim, Germany*
[f] *Department of Dermatology, Center for Dermatooncology, University Hospital Tübingen, Germany*
[g] *Department of Dermatology and Allergy, University Hospital of Munich, Munich, Germany*
[h] *Department of Dermatology, University of Luebeck, Luebeck, Germany*
[i] *Department of Dermatology, Klinikum Ludwigshafen, Ludwigshafen, Germany*
[j] *Skin Cancer Centre, Department of Dermatology and Allergy, Hannover Medical School, Hannover, Germany*
[k] *Department of Dermatology, Medical Center – University of Freiburg, Faculty of Medicine, University of Freiburg, Germany*
[l] *Department of Dermatology, University Hospital Erlangen, Friedrich-Alexander-University Erlangen-Nürnberg, Erlangen, Germany*
[m] *Department of Radiotherapy, West German Cancer Center, University Hospital, University of Duisburg-Essen and the German Cancer Consortium (DKTK) University of Duisburg-Essen, Essen, Germany*
[n] *Max-Eder Research Group for Pediatric Sarcoma Biology, Institute of Pathology, Faculty of Medicine, LMU Munich, Germany*
[o] *German Cancer Consortium (DKTK), Partner Site Munich, Munich, Germany*
[p] *German Cancer Research Center (DKFZ), Heidelberg, Germany*

Received 21 November 2018; received in revised form 22 December 2018; accepted 29 December 2018
Available online 2 February 2019

* *Corresponding author*: University Hospital Essen, Department of Dermatology, Hufelandstrasse 55 45147 Essen, Germany. Fax: +49 201 723 6842.
E-mail address: alexander.roesch@uk-essen.de (A. Roesch).

https://doi.org/10.1016/j.ejca.2018.12.024

KEYWORDS
Melanoma;
Radiotherapy;
Targeted therapy;
Resistance;
Cross-resistance;
Therapy sequencing;
Slow-cycling cells;
JARID1B/KDM5B;
Repopulation

Abstract ***Introduction:*** Treatment of patients with metastatic melanoma is hampered by drug-resistance and often requires combination with radiotherapy as last-resort option. However, also after radiotherapy, clinical relapses are common.
Methods & results: Our preclinical models indicated a higher rate of tumour relapse when melanoma cells were first treated with $BRAF^{V600E}$ inhibition (BRAFi) followed by radiotherapy as compared to the reverse sequence. Accordingly, retrospective follow-up data from 65 stage-IV melanoma patients with irradiated melanoma brain metastases confirmed a shortened duration of local response of mitogen-activated protein kinase (MAPK)-inhibitor–pretreated compared with MAPK-inhibitor–naïve intracranial metastases. On the molecular level, we identified JARID1B/KDM5B as a cellular marker for cross-resistance between BRAFi and radiotherapy. $JARID1B^{high}$ cells appeared more frequently under upfront BRAFi as compared with upfront radiation. JARID1B favours cell survival by transcriptional regulation of genes controlling cell cycle, DNA repair and cell death.
Conclusion: The level of cross-resistance between combined MAPK inhibition and radiotherapy is dependent on the treatment sequence. JARID1B may represent a novel therapy-overarching resistance marker.

1. Introduction

Cutaneous melanoma is the most aggressive form of skin cancer, and once it metastasises, survival rates dramatically drop [1]. Systemic therapy of advanced melanoma greatly improved with the approval of small molecule kinase inhibitors of mitogen-activated protein kinase (MAPK) signalling (mutated in ~70–80% of patients) and immune checkpoint blockers [1]. However, metastatic melanoma is still associated with a poor overall survival [1], largely because of the presence and/or rapid emergence of drug resistance across surviving melanoma cells, particularly in MAPK inhibitor (MAPKi)-treated patients [2].

Moreover, deadly systemic melanoma progression is associated with development of anatomically critical metastases that require immediate therapy intervention, particularly in the brain (affecting ~40–50% of stage IV melanoma patients [3]). Owing to the imminent threat in such individuals, oncologists worldwide feel obliged to enhance the existing intracranial activity of MAPK-targeted agents or immune checkpoint blockers by combination with radiotherapy protocols. A number of retrospective analyses and also first clinical trials indicate favourable outcomes and acceptable toxicities of such combination therapies [4–10], but there are no data available that systematically addresses the effect of therapy sequencing on the durability of clinical responses and development of therapy overarching resistance (cross-resistance). A prime example of how important therapy timing will become in the clinical routine has been recently demonstrated by Hugo *et al.* Their findings have suggested that melanomas with acquired clinical resistance to MAPKi recurrently lose CD8 T-cell numbers and antigen presentation functions, which points to cross-resistance to anti-PD1/PD-L1 immunotherapy [11]. Moreover, this observation could indicate that once melanoma cells have acquired the MAPKi-resistant phenotype, they may be resistant against any exogenous stressor including also ionising radiation.

A number of genetic and phenotypic molecular mechanisms of therapy resistance have been identified in melanoma under MAPKi treatment [2,12–14]. The most common include genetic alterations in for example BRAF, NRAS and MEK as well as epigenetically driven adaptive plasticity of melanoma cell subpopulations. Yet, it is not fully understood how some melanoma cells escape initial therapeutic hits including radiation-induced killing. Our lab has previously described the existence of a small subpopulation of slow-cycling cells that survives multiple available drugs and significantly repopulates melanomas, irrespective of the genetic background of the melanomas analysed [15,16]. This multidrug-resistance seems to be dependent on a high expression level of the histone H3K4 demethylase JARID1B/KDM5B (Jumonji AT-rich interactive domain 1B/lysine-specific demethylase 5B) [15,17,18]. In the therapeutic context *in vitro*, *in vivo* and in patients, melanoma cell populations that survive therapies have been shown to be significantly enriched for the $JARID1B^{high}$ cell phenotype [15,17,18]. In a recently published paper, Bayo *et al.* showed that the inhibition of JARID1B sensitises lung cancers to radiation *in vitro* and *in vivo*, through the involvement of JARID1B in the cellular response to double-strand breaks [19].

Based on JARID1B's role in multidrug resistance and tumour maintenance in melanoma, we now examined its applicability as a universal resistance marker also to radiotherapy and implemented this idea into a novel

preclinical test platform for outcome prediction of radiotherapy combination sequences. As a proof of concept, we assessed the levels of cross-resistance between $BRAF^{V600E}$ inhibition (BRAFi) and radiotherapy and examined the molecular mechanisms downstream of JARID1B that mediate cell survival.

2. Materials and methods

2.1. Cell culture, reagents, in vitro radiation, siRNA and shRNA constructs

Human melanoma cell lines were provided by M. Herlyn (The Wistar Institute, Philadelphia, USA) or commercially acquired. For details see, Supplementary Table 1, [15,43]. In brief, WM3734 and WM9 cells were established from human metastases of melanoma and are both $BRAF^{V600E}$ and *NRAS* wt, while MelJuSo was established from a primary human melanoma and is *BRAF* wt and $NRAS^{Q61L}$. Cells were cultured with 2% foetal bovine serum (FBS)-substituted melanoma medium (Tu2%) as previously described [44] and grown at 37°C in 5% CO_2. Radiation was performed at room temperature with an X-ray machine (Precision X-Ray Inc., North Branford, CT) operated at 320 kV, 12.5 mA with a 1.65 mm Al filter, at a distance of 50 cm and a dose rate of 3.71 Gy/min. Cells were returned to the incubator immediately after exposure to ionising radiation. PLX4720 (Cat # S1152) and GSK2118436—referred to as GSK436 throughout the manuscript—(Cat # S2807) were purchased from Selleckchem (Munich, Germany). All compounds were stored at −20°C in dimethyl sulfoxide (DMSO) as 10 mM stocks. JARID1B siRNA (5′ −A CGCACCAAGCCGAAAGTAAA-3′) was purchased from Qiagen (Hilden, Germany) and transfected (8 nM) using jetPRIME® Polyplus according to the manufacture's protocol. Knockdown efficiency was determined by Western blot analysis and quantitative PCR (QPCR). A 'non-functional' siRNA clone (Cat #SI00090314, did not affect JARID1B expression) was used as a control. Tet-3GshJARID1B doxycycline-inducible vectors were generated according to the publicly available protocol of Wiederschain *et al.* [45], using Tet-pLKO-puro (Plasmid# 21 915, Addgene, Cambridge, MA, USA) as a backbone. The melanoma cell line WM3734 was transfected either with a non-targeting shRNA (5′-CAACAAGATGAAGAGCACCAA-3′) termed $WM3734^{Tet3G-Scr}$ or with shRNA targeting *JARID1B* (5′-ACGCACCAAGCCGAAAGTAAA-3′) termed $WM3734^{Tet3G\text{-}shJARID1B}$.

The first treatment sequence applied radiation (IR) followed by $BRAF^{V600E}$-selective inhibition [PLX4720 or GSK2118436 (TT)], while the second sequence started in the reverse order, i.e., BRAFi followed by radiation. In brief, once WM3734 melanoma cells reached ~70% confluence, the cells were either irradiated at day 0, then treated with BRAF inhibitors (PLX4720 or GSK436) at day 3 (IR → TT) or vice versa (TT → IR). The cell numbers used for the assays and the temporal sequences were designed in such a way that cell density effects could be excluded as good as possible. As readout, the JARID1B expression level was assessed on day 6 and total cell counts on day 9. The PLX4720 and GSK436 concentrations were chosen based on preceding drug titration assays particularly considering the JARID1B enrichment to ensure an ideal read-out for this proof-of-principle approach. PLX4720 [0.2 μM] and GSK436 [3 nM] were the concentrations resulting in the highest JARID1B enrichment as determined by J/EGFP flow cytometry in $WM3734^{JARID1Bprom-EGFP}$ cells.

2.2. Patient tissue samples and clinical data collection

Immunohistochemical staining of the 17 archived human melanoma samples was approved by the ethics committees of the contributing clinical skin cancer centres according to local informed consent protocols (Essen 16-7191-BO and 11-4715, Dresden EK59032007, Mannheim 2014-835R-MA, Tübingen 494/2017BO2). The retrospective data analysis of 65 stage IV melanoma patients with brain metastases who received radiotherapy plus MAPKi was collaboratively done within the German DeCOG network based on local patient records (contributing sites: Dresden, Mannheim, Munich, Tübingen, Lübeck, Hannover, Freiburg and Essen). Multicentric data collection was approved by the ethics committee of the leading centre (Dresden EK270062016). All patients received BRAF and/or MAP kinase (MEK) inhibitors within 6 weeks of radiotherapy. There were 26 females and 39 males, and the median age was 58 years (range, 29–87 years). For further details, see Supplementary Table 2.

2.3. Flow cytometry

Flow cytometric detection of double staining of JARID1B expression levels and Live/Dead® (ThermoFisher Scientific, Oberhausen, Germany) was performed using a Gallios flow cytometer (Beckman Coulter, Krefeld, Germany) following standard protocols. In brief, cells were stained with Live/Dead® for 30 min at 4°C, fixed in 2% formalin with 0.1% Triton X-100 in phosphate buffered saline (PBS) for 20 min at room temperature (RT) and then permeabilised in 90% methanol for 30 min at −20°C. For detection of endogenous JARID1B protein, primary (NB100-97821, Novus Biologicals, Colorado, USA) and secondary (Alexa Fluor® 568 goat anti-rabbit IgG (H + L), Life Technologies, Orlando, USA) antibodies were incubated for 30 min at RT at a dilution of 1:1200. Before and after antibody incubation, cells were washed with FACS buffer (0.5 M ethylene diamine tetra-acetic acid [EDTA], 1% FBS, 1× PBS). Data were analysed using FlowJo, V7.6.5 (Tree Star,

Ashland, OR, USA). For assessment of endogenous JARID1B expression, an analytical threshold was set to 1% of the isotype control. Experiments were performed as three independent replicates. Assessment of JARID1B expression by the human JARID1B-promoter-EGFP (enhanced green fluorescent protein)-reporter construct in WM3734$^{JARID1Bprom-EGFP}$ cells was done as described previously [15,16].

2.4. Proliferation, cell cycle and apoptosis assays

Trypan blue and crystal violet staining were performed to assess cell numbers and viability according to common standard protocols. In short, cells were seeded in 24-well plates and allowed to proliferate to ~70% confluence. Trypan blue-negative living cells were counted using a haemocytometer. For crystal violet staining, the cell culture medium was removed; the cells were washed and fixed with 70% ethanol for 1 h at RT and then stained with 1% crystal violet for 30 min. The cells were washed with tap water and dried on filter paper. After the plates were photographed, the dye was dissolved in 70% ethanol and emission was measured at 550 nm using an Epoch Microplate Spectrometer (BioTek, Winooski, VT, USA). The images were also quantified using the ImageJ-win64 software. Three independent experiments were performed, and standard deviation (SD) was calculated. Propidium iodide staining for cell cycle analysis was performed as previously described (Roesch *et al.*, 2010). In brief, melanoma cells were seeded in 6-cm plates and allowed to proliferate to ~70% confluence. The cells were then irradiated with 0, 5 or 10 Gy. After 1, 3 or 6 days, cells were trypsinised and washed with PBS containing 5 mM EDTA. After incubation with 100% ethanol, RNase A was added. Propidium iodide was added to a final concentration of 100 μg/mL, and intercalation into chromosomal DNA was measured using a Gallios cytometer (Beckman Coulter). Data were analysed using FlowJo software (version 7.6.5). Dead cells (sub-G1) have been gated out.

2.5. Western blot

Proteins were extracted as described previously [46], and 20 μg of cell extract was separated on a 10% polyacrylamide-sodium dodecyl sulphate gel before being transferred onto a membrane (Roth, Karlsruhe, Germany). Primary antibodies were incubated at 4°C overnight in Tris-buffered saline containing 0.1% Tween-20 and 5% milk. Primary antibodies were rabbit anti-JARID1B 1:1200 (NB100-97821), Rb (Cell Signaling, Cat# 9309) and Tubulin (Cell Signaling, Cat# 2148). Then the blots were washed with TBST and incubated for 1 h with either anti-rabbit (115-035-046) or anti-mouse (115-035-003) horseradish peroxidase–conjugated secondary antibody (Jackson Immuno Research Laboratories Inc., Missouri, USA) diluted 1:10 000 in tris buffered saline Tween 20 (TBST)-milk 5%. Western blots were visualised using the enhanced chemiluminescence system (WesternBright Chemiluminescence Substrate, Biozym, Hessisch Oldendorf, Germany). The western blots were scanned using the LAS300 Imaging System (Fuji, Munich, Germany). For quantification, signals were densitometrically normalised to tubulin with ImageJ-win64 software.

2.6. QPCR

RNA was isolated using the RNeasy Mini Kit according to the manufacturer's protocol (Qiagen, Hilden, Germany). The primer sequences for JARID1B detection have been published previously (Roesch *et al.*, 2010). 20 ng RNA and 0.1 nM primers were used together with Precision Onestep qRT-PCR master mix (PrimerDesign, UK) for the evaluation of JARID1B and 18S housekeeping gene expression. A negative control without RNA was run in each assay. Amplifications were performed in a StepOneplus™ detection system (Applied Biosystems, CA, USA). Thermal cycler conditions for all genes were 95°C for 20 min, then 40 cycles of 3 min at 95°C, followed by 30 s at 60°C. All experiments were performed at least in triplicates. Baseline and threshold values were set using the StepOneplus™ software. mRNA expression was calculated using the standard curve method according to the Applied Biosystem's Guide. Expression ratios of controls were normalised to 1.

2.7. Mouse in vivo studies

Mouse experiments were performed in strict accordance with the recommendations of the Guide for the Care and Use of Laboratory Animals of the German Government, which was approved by the Committee on the Ethics of Animal Experiments of the responsible authorities [Landesamt für Natur, Umwelt und Verbraucherschutz (LANUV), Regierungspräsidium Düsseldorf Az. 84–02.04.2012.A246; Az.84–02.04.2013.A092]. Immunodeficient NMRI-(nu/nu)-nude mice were purchased from the University Hospital Essen (age 6–12 weeks). Animals were housed in an individually ventilated cage rack system (Techniplast, Italy) and were fed with sterile high calorie laboratory food (Ssniff, Germany). Drinking water was supplemented with chlorotetracycline and potassium sorbate acidified to a pH of 3.0 with hydrochloric acid and was provided *ad libitum*. Xenograft tumours of the human melanoma cell line WM3734 were generated by injection of 2×10^5 cells in 50 μl medium [1:2 mixture of Tu2% with Matrigel® (BD Biosciences)] into the hind leg. Radiation started at an average tumour volume of 100 mm^3. Mice were randomised into two groups/cell line (0 Gy and 10 Gy). Mice were anesthetised (2% isoflurane), and tumours were exposed to a single dose of 10 Gy ± 5% in 5 mm tissue depth (~1.53 Gy/min, 300 kV, filter: 0.5 mm Cu, 10 mA, focus distance: 60 cm) using a

collimated beam with a XStrahl RS 320 cabinet irradiator (XStrahl Limited, Surrey, UK). Tumour growth was measured twice weekly using a caliper, and volume was calculated according to the formula $V = (W X D X H)/2$ [mm^3]. Tumour samples were either snap frozen in liquid nitrogen for subsequent protein analyses or fixed in formalin for histological assessment and immunostaining. For the mouse data in Fig. 2, we performed two *in vivo* experiments. In the first experiment, we xenografted WM3734 melanoma cells into nude mice (n = 28, 200 000 cells/mouse) and radiated half of the mice (n = 14) with a single dose of 10 Gy, when the tumours reached a volume of ~100 mm^3. The dose was chosen based on our *in vitro* observation that 10 Gy resulted in a more persistent increase of JARID1B. The remaining 14 mice served as non-irradiated controls. Seven tumours of the controls and seven of the irradiated mice were collected on day 34 (early time point). The rest of the mice (7 controls and 7 irradiated) were collected on day 48 (intermediate time point, p = 0.013). In the second experiment, seven mice were irradiated, and seven served as non-irradiated controls. The tumours were collected when they reached a maximum volume of ~1000 mm^3 at day 48 for the controls and at day 58 for the radiated mice (late time point).

2.8. Immunostaining and immunohistochemistry

For JARID1B and Ki-67 coverslip staining, the cell culture medium was removed; the cells were washed and fixed with 2% PFA (paraformaldehyde) (+0.1% Triton X-100) for 20 min at RT and then blocked with 5% bovine serum albumin (+0.1% Triton X-100) for 30 min. Then, the cells were washed with PBS (+0.1% Triton X-100), and primary antibody was added for 30 min at RT. Subsequently, the Dako REAL™ Detection System (Dako, Glostrup, Denmark) was used according to the manufacturer's instructions. The cover slips were mounted on a glass slide using Dako Mounting Media. For immunohistochemical staining of FFPE tissue samples, tissues were fixed in 10% formalin, dehydrated and embedded in paraffin and followed the manufacturer's protocol (Dako REAL™ Detection System) as described previously [30]. Samples were evaluated using Zeiss AxioObserver.Z1 microscope at 20× and 40× magnification. For JARID1B assessment, a nuclear staining–intensity score was designed, where 0 is no staining and 4.0 is a very high staining (meaning intensity of >75% of cells showing red nuclear staining, indicating JARID1B staining). The staining was assessed by two independent investigators in a blinded fashion (A.R. and F.V.). Immunoreactivity was scored using uniform criteria to maintain the reproducibility of the method.

2.9. The cancer genome atlas and gene ontology

The gene analysis shown here is based on the cancer genome atlas (TCGA) generated data (http://cancergenome.nih.gov/). TCGA skin cutaneous melanoma data have been accessed and downloaded via cBioPortal (http://www.cbioportal.org/). Gene ontology (GO) analysis was performed using the GSEA software (http://software.broadinstitute.org/gsea). The software identifies the top 100 significantly regulated pathways with regards to the gene(s) in question.

2.10. Statistical analyses

The student's *t*-test was used to evaluate mean differences between groups. Error bars are defined in the figure legends. Fisher's exact test was used to assess the correlation between therapy sequences and response to treatment in patients. One-way analysis of variance (ANOVA) was used to test the association between Gy doses and cell cycle. Statistical tests were performed using GraphPad Prism (version 6.0), conducted at the two-sided significance level, where p-values of less than 0.05 were considered significant.

3. Results

3.1. In vitro modeling of radiation-resistance in melanoma

To model cell survival in melanoma following radiation (IR), we setup a cell culture–based system that allowed the adjustment of radiation doses and evaluation of the radiation-resistant melanoma cell population. The radiation doses used in our model were selected based on previous cell culture experiments, where differences between IR-resistant and IR-sensitive tumour cells were observed at a dose of 5 Gy or higher [20]. Consequently, WM3734 cells, a typical $BRAF^{V600E}$-carrying melanoma cell line, were irradiated with either 5 or 10 Gy, and the remaining cell fraction was quantitated by crystal violet staining on day 3 and day 6 after radiation (Fig. 1A). As expected, there was a significant dose-dependent, mostly cytostatic decrease in total cell numbers. Higher, more cytotoxic radiation doses were avoided because of the limited controllability of delayed radiation-induced cell death, which would particularly hamper the subsequently planned drug combination experiments. Accordingly, we observed a dose-dependent increase in the G2/M phase of the cell cycle and a loss of Ki-67 staining after radiation (Fig. 1B and C), which is consistent with radiation-associated cell-cycle arrest as reported by others [21–23].

Since previous work from us and others has shown that multitherapy-resistant melanoma cells [15,16,24] and radiation-resistant fibroblasts [25] were both associated with elevated expression of the H3K4 demethylase JARID1B/KDM5B, we wondered if the cell-cycle–arrested radiation-resistant melanoma cell fraction observed in our model is also enriched for JARID1B. Using a

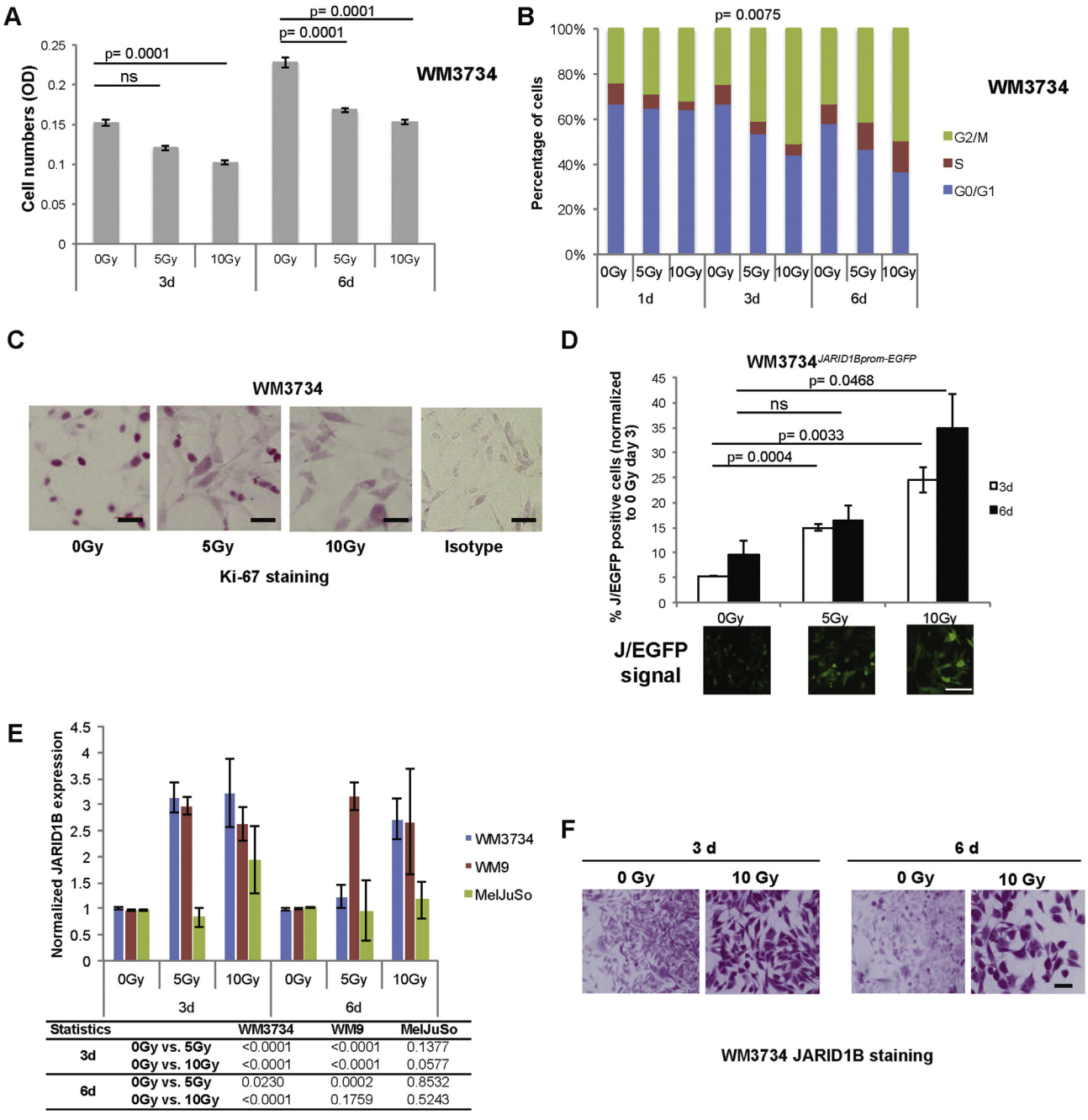

Statistics		WM3734	WM9	MelJuSo
3d	0Gy vs. 5Gy	<0.0001	<0.0001	0.1377
	0Gy vs. 10Gy	<0.0001	<0.0001	0.0577
6d	0Gy vs. 5Gy	0.0230	0.0002	0.8532
	0Gy vs. 10Gy	<0.0001	0.1759	0.5243

Fig. 1. **Cell cycle arrest and JARID1B enrichment after radiation treatment *in vitro*.** (A) Crystal violet assay of WM3734 melanoma cells following 0, 5 or 10 Gy irradiation for 3 and 6 days. (B) Propidium iodide-based cell cycle analysis of WM3734 melanoma cell lines 1, 3 or 6 days after 0, 5 or 10 Gy irradiation. Statistical significance for the G2/M phase across Gy doses and days of treatment was analysed by one-way ANOVA. (C) Ki-67 staining of WM3734 melanoma cells at 6 days after irradiation with 0, 5 or 10 Gy. Scale bar represents 100 μm. (D) Flow cytometry analysis showing the percentage of J/EGFP-positive cells in WM3437$^{JARID1Bprom-EGFP}$ cells 3 and 6 days following 0, 5 or 10 Gy irradiation. Representative images of J/EGFP-positive cells (6 days postradiation) are shown below the corresponding radiation dose. (E) Antibody-based flow cytometry analysis of JARID1B protein expression 3- and 6-days following irradiation with 5 or 10 Gy. Results were normalised to the respective 0 Gy values for each cell line. Statistical significance was confirmed by one-way ANOVA, which shows the overall significance between each cell line (p values indicated in table under figure). (F) Immunostaining of JARID1B in WM3734 melanoma cells at days 3 and 6 following either 0 or 10 Gy irradiation. Scale bars represent 100 μm. Error bars represent SD from three independent experiments (A, B, D, E).
ANOVA, analysis of variance.

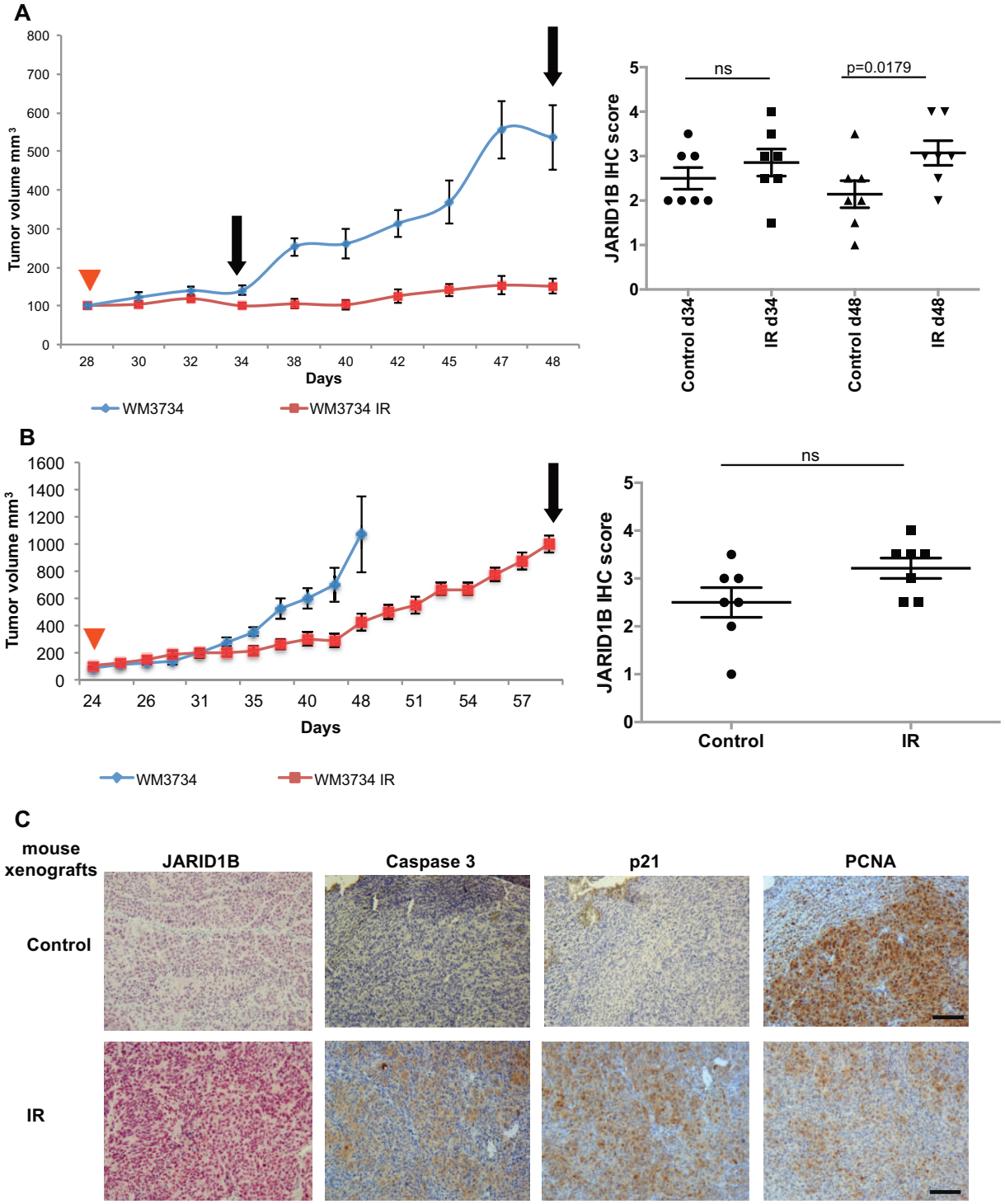

Fig. 2. **Radiation-depended JARID1B enrichment in a melanoma mouse xenograft model.** (A) *Left:* Nude mice were xenotransplanted with WM3734 melanoma cells, and tumours were radiated with 10 Gy when they reached a volume of ~100 mm^3 (red triangle). Tumour volumes were measured twice a week (n = 14 mice/group, 2 groups, i.e., control and irradiated). At day 34 and day 48 (black arrows), seven mice of each group were sacrificed, and JARID1B expression was assessed in explanted melanomas by immunohistochemistry (IHC). JARID1B staining was scored from 0.0 (no staining) to 4.0 (high intensity staining). *t*-Test was performed between the mouse groups at the last measurement on day 48 (p = 0.013). *Right:* Scatter plot representing the JARID1B IHC score in the different mouse groups. (B) Nude mice were xenotransplanted and irradiated as indicated in (A), n = 7 mice/group, but sacrificed at a later time point, when tumours reached a maximum volume of ~1000 mm^3 (controls day 48, irradiated day 58). (C) Representative images of IHC staining's from intermediate time point xenografts of JARID1B, caspase 3, p21 and PCNA. Scale bar represents 100 μm.

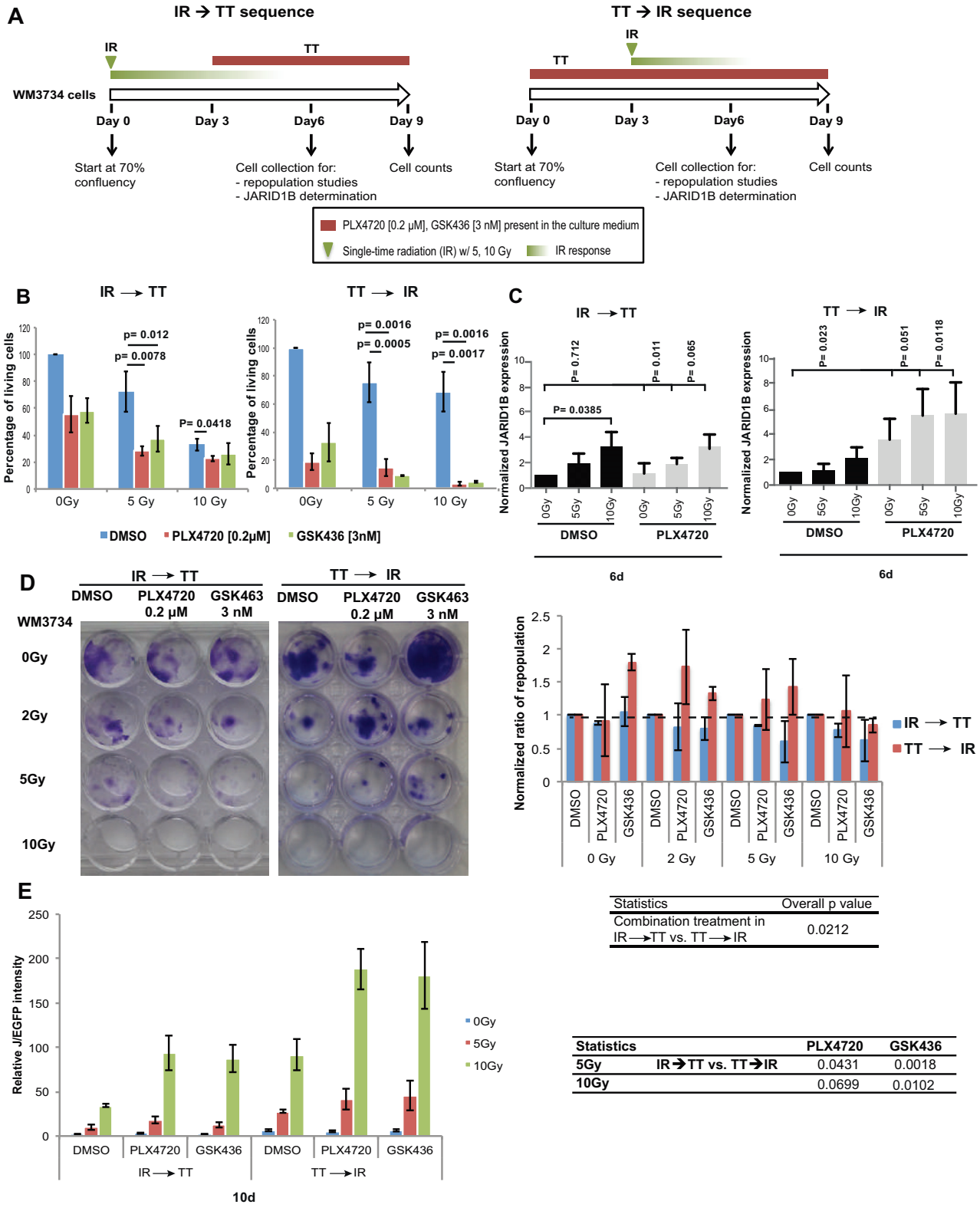

Statistics	Overall p value
Combination treatment in IR→TT vs. TT→IR	0.0212

Statistics		PLX4720	GSK436
5Gy	IR→TT vs. TT→IR	0.0431	0.0018
10Gy		0.0699	0.0102

Fig. 3. **Combination effects of radiation therapy and targeted BRAF^{V600E} inhibition on melanoma cell elimination and tumour repopulation.** (A) *Left:* Schematic diagram detailing the flow of the treatment sequence IR (radiation) → TT (targeted therapy), where cells are treated with increasing doses of IR (0, 5 or 10 Gy) followed by a fixed dose of TT (PLX4720 [0.2 μM] or GSK436 [3 nM]). *Right*. Reverse treatment sequence TT → IR. (B) Overall melanoma cell killing was assessed by WM3734 cell counts using trypan blue at day 9, following either IR → TT or TT → IR. Error bars represent SD from three independent experiments. *t*-Test shows a significant decrease in the percentage of living cells ($p \leq 0.01$). (C) Flow cytometric determination of the live JARID1B expressing cell subpopulation in WM3734 cells on days 6 and 9 following the indicated treatment (complete live/dead data set is shown in Supplementary Fig. 2). Results were normalised to the

JARID1B-promoter-EGFP-reporter construct [15,16], we could detect a statistically significant dose-dependent enrichment for JARID1B-driven EGFP expression in WM3734 cells after radiation (Fig. 1D). To validate this observation, two additional melanoma cell lines, WM9 and MelJuSo representing different genetic backgrounds (Supplementary Table 1), were analysed for their endogenous JARID1B protein levels after radiation. Flow cytometric quantitation confirmed a strong JARID1B protein enrichment in WM3734 and WM9 cells with a less prominent effect in MelJuSo cells (Fig. 1E). The discrepancy between the different melanoma cell lines was possibly because of their different growth kinetics (Supplementary Table 1). The elevated JARID1B expression after radiation was additionally confirmed on the subcellular level by anti-JARID1B immunostaining (WM3734 cells shown as an example in Fig. 1F).

In sum, our observations suggest a dose-dependent increase of JARID1B expression in the radiation-resistant fraction of melanoma cells *in vitro*. Since JARID1B expressing cells are highly capable of tumour repopulation [15], they may represent a critical source of melanoma relapses after radiation therapy. However, it was unclear at this point, if the JARID1B expression also changes *in vivo* and in patients following radiation.

3.2. JARID1B marks radiation-resistant melanoma cells in vivo

Based on our *in vitro* observations, our next step was to longitudinally assess the enrichment for JARID1B^{high} melanoma cells also *in vivo* at different time points after radiation. Therefore, we designed two *in vivo* experiments, where we investigated JARID1B expression at an early (day 34), intermediate (day 48) (Fig. 2A) and late time point (day 58) (Fig. 2B) after radiation. The later time point tumours were collected when the tumours gained the ability to 're-grow' after radiation (Fig. 2B). Then, we assessed the endogenous JARID1B protein expression in the collected tumours using immunohistochemistry and designed a nuclear staining–intensity score, where 0 indicated no staining and 4.0 very high staining (Fig. 2A and B, right panels, Fig. 2C left panel). Interestingly, at day 34, when radiated and control tumours still had comparable sizes, i.e., before the proliferation phase of the controls has started, the selection for the surviving JARID1B^{high} subpopulation had not yet reached statistical significance. At day 48, JARID1B-enrichment became statistically significant. At day 58, when the surviving cells in the radiation group had fully repopulated the tumours, the statistical significance vanished again. Also, this phenomenon matches previous observations showing that JARID1B^{high} melanoma cells maintain tumour growth by reconstituting the original tumour heterogeneity and that the JARID1B phenotype can be transient [15]. Furthermore, we stained the tumours collected from the intermediate time point for proliferation (PCNA, proliferating cell nuclear antigen), cell cycle arrest (p21) and apoptosis (caspase 3) markers (Fig. 2C). Indeed, the irradiated tumours showed a decrease in PCNA that was paralleled by an increase in p21 and caspase 3 expression levels as compared with the non-irradiated controls.

3.3. Sequence-dependent levels of cross-resistance between BRAF^{V600E} inhibition and radiotherapy in melanoma

Anatomically critical melanoma metastases, e.g. in the brain, often require immediate tumour control and are commonly treated with combined signalling-targeted plus radiation therapy [1]. To further explore whether the JARID1B-associated multitherapy-resistant cell phenotype is also enriched under such combination regimens, we designed two experimental treatment protocols *in vitro* resembling two scenarios that are commonly occurring in daily clinical routine (see Materials and Methods for more details). In brief, the first treatment sequence applies radiation (IR) followed by BRAF^{V600E}-selective inhibition (PLX4720 or GSK2118436 [TT]) (Fig. 3A, right panel). The second sequence started in the reverse order, i.e., BRAFi followed by radiation (left panel). Targeted therapy drug concentrations were based on results in Supplementary Fig. 1A and 1B (see Materials and Methods for more details). As expected, both treatment sequences had an additive effect on the cell killing efficiency (Fig. 3B). However, despite the significant reduction in cell numbers, still ~20% of cells were able to survive in the IR → TT sequence (left panel) and ~5% in the TT → IR sequence (right panel) indicating that also those combination regimens did not kill all melanoma cells.

Next, we assessed the JARID1B expression in flow cytometry assays following the combination treatment in both sequences (Fig. 3C). Interestingly, pretreatment of melanoma cells with PLX4720 ahead of radiation

DMSO at 0 Gy for each day. Error bars represent SD from three independent experiments. (D) *Left:* Tumour cell repopulation capacity of pretreated cells as assessed by crystal violet staining. WM3734 cells were co-treated as indicated, harvested on day 6, and the surviving cells were re-seeded (600 cells/well in 24-well plates). Cells were then allowed to repopulate for 3 additional weeks. *Right:* Quantification of crystal violet staining. The values were normalised to the DMSO control (set as 1) of each treatment group. Statistical significance was confirmed by one-way ANOVA. (E) Flow cytometry analysis of the J/EGFP-positive subpopulation after WM3437$^{JARID1Bprom-EGFP}$ cells were treated the same way, re-seeded (10,000 cells/well in 6-well plates) and analysed after another 4 days. The J/EGFP signal intensity was normalised to the cell number upon cell collection. Statistical significance was performed using one-way ANOVA to determine the overall significance between treatment groups. The p values < 0.05 were considered significant.
ANOVA, analysis of variance.

A

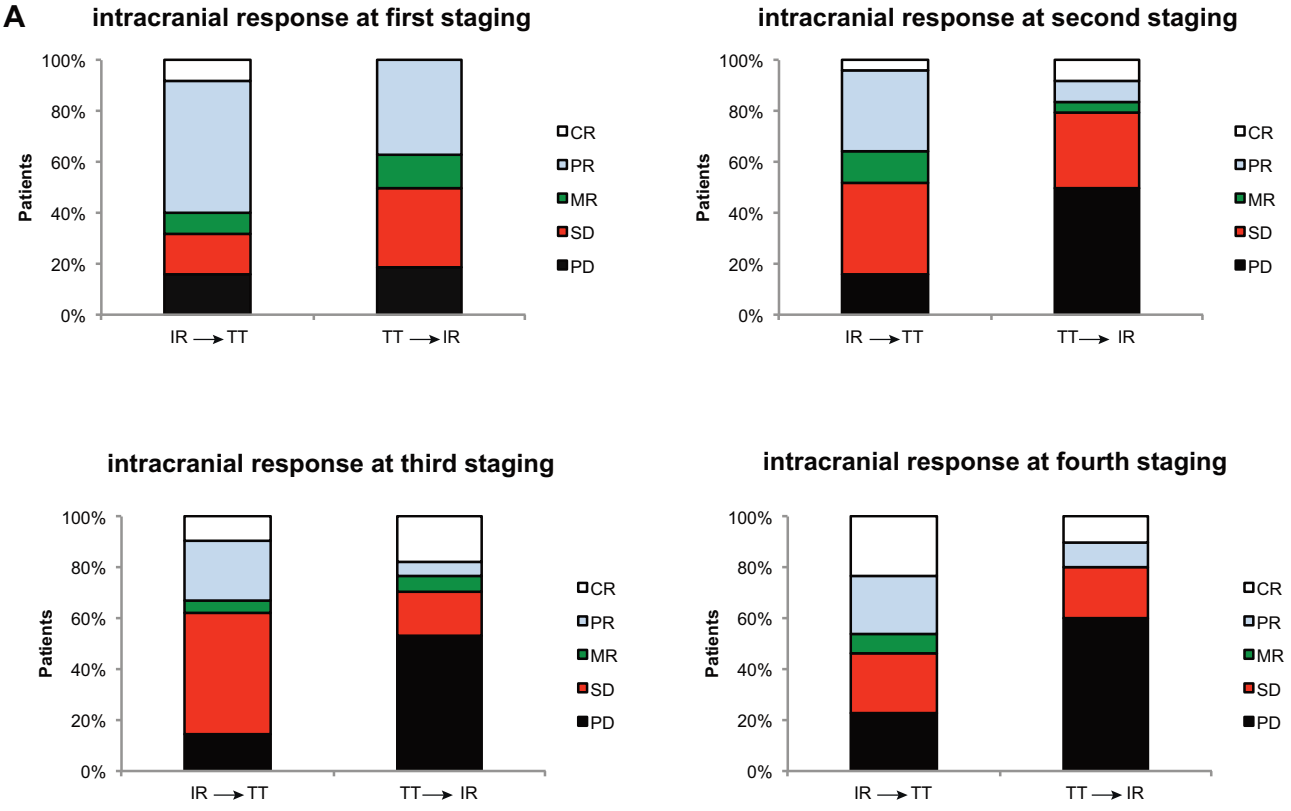

B

	PD			
Statistics	**1st staging**	**2nd staging**	**3rd staging**	**4th staging**
IR → TT vs. TT → IR	1.00	0.0157	0.0159	0.1023

C

	Treatment sequence	PD	SD	MR	PR	CR	Total number of patients
Intracranial response at first staging	**IR → TT**	4	4	2	13	2	25
	TT → IR	6	10	4	12	0	32
Intracranial response at second staging	**IR → TT**	4	9	3	8	1	25
	TT → IR	12	7	1	2	2	24
Intracranial response at third staging	**IR → TT**	3	10	1	5	2	21
	TT → IR	9	3	1	1	3	17
Intracranial response at fourth staging	**IR → TT**	3	3	1	3	3	13
	TT → IR	6	2	0	1	1	10

Fig. 4. **Intracranial responses of stage IV melanoma patients depend on the sequence of radiotherapy and MAPKi.** (A) Radiologic intracranial response at 1st, 2nd, 3rd and 4th staging for both therapy sequences. Stable disease (SD), progressive disease (PD), partial response (PR), complete response (CR) and mixed response (MR). The data are shown as the percentage of the total number of patients per treatment group and staging time point. (B) Statistical significance is shown for PD between IR → TT and TT → IR patients using Fisher's exact test. (C) Absolute patient numbers of panel (A).
MAPKi, MAPK inhibition; TT, targeted therapy; IR, radiation.

resulted in a higher relative enrichment for alive JARID1B^{high} cells (Fig. 3C is an extract of the data for WM3734 cells from Supplementary Figure 2A, which shows the complete data of live/dead JARID1B double-staining for all three cell lines, Supplementary Fig. 2B and 2C). Cells were gated as either: JARID1B^{high}/live, JARID1B^{high}/dead, JARID1B^{low}/live and JARID1B^{low}/dead. The same experiment was performed in WM9 and MelJuSo (Supplementary Fig. 2B and 2C), where comparable effects of JARID1B enrichment were observed in *BRAF*^{V600E}-driven WM9 9 days after start of treatment, but as expected, not in *BRAFwt* MelJuSo cells.

Since our former findings suggest that JARID1B^{high} cells have a high potential to re-establish tumour growth [15]; in the next experiment, WM3734 cells were sequentially co-treated as indicated above, and surviving cells

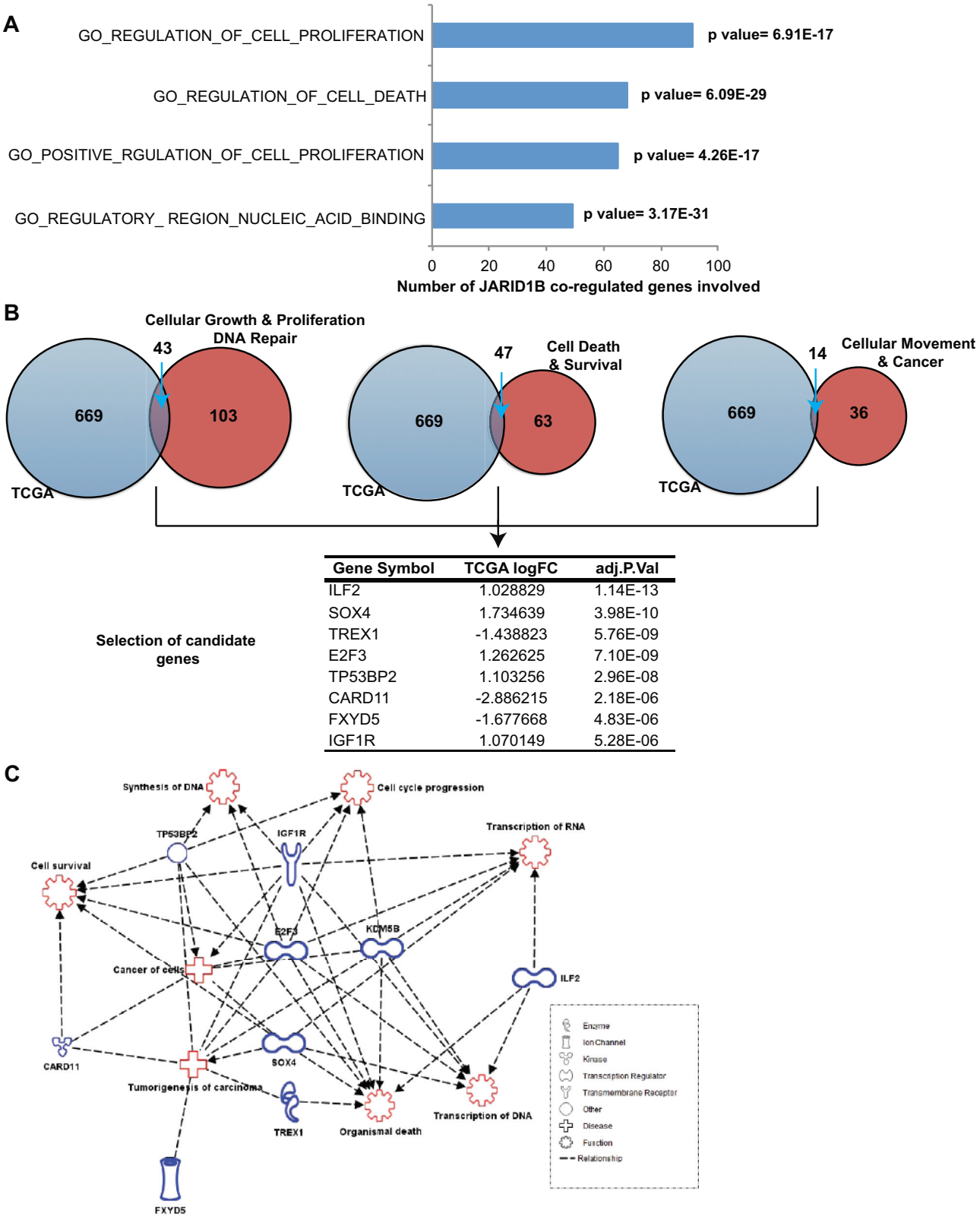

Gene Symbol	TCGA logFC	adj.P.Val
ILF2	1.028829	1.14E-13
SOX4	1.734639	3.98E-10
TREX1	-1.438823	5.76E-09
E2F3	1.262625	7.10E-09
TP53BP2	1.103256	2.96E-08
CARD11	-2.886215	2.18E-06
FXYD5	-1.677668	4.83E-06
IGF1R	1.070149	5.28E-06

Fig. 5. **JARID1B affects cell survival in melanoma.** (A) Subset of cell survival-associated gene ontology (GO) pathways that have been identified based on JARID1B co-regulated transcripts in human melanoma. (B) Overlap between JARID1B-co-regulated genes found in TCGA and Ingenuity™ networks that control the indicated survival-relevant cellular processes. The table indicates 8 selected candidate genes from the overlap of the Venn diagrams. (C) Ingenuity™ network directly interconnecting JARID1B-co-regulated genes with survival-relevant cellular processes.

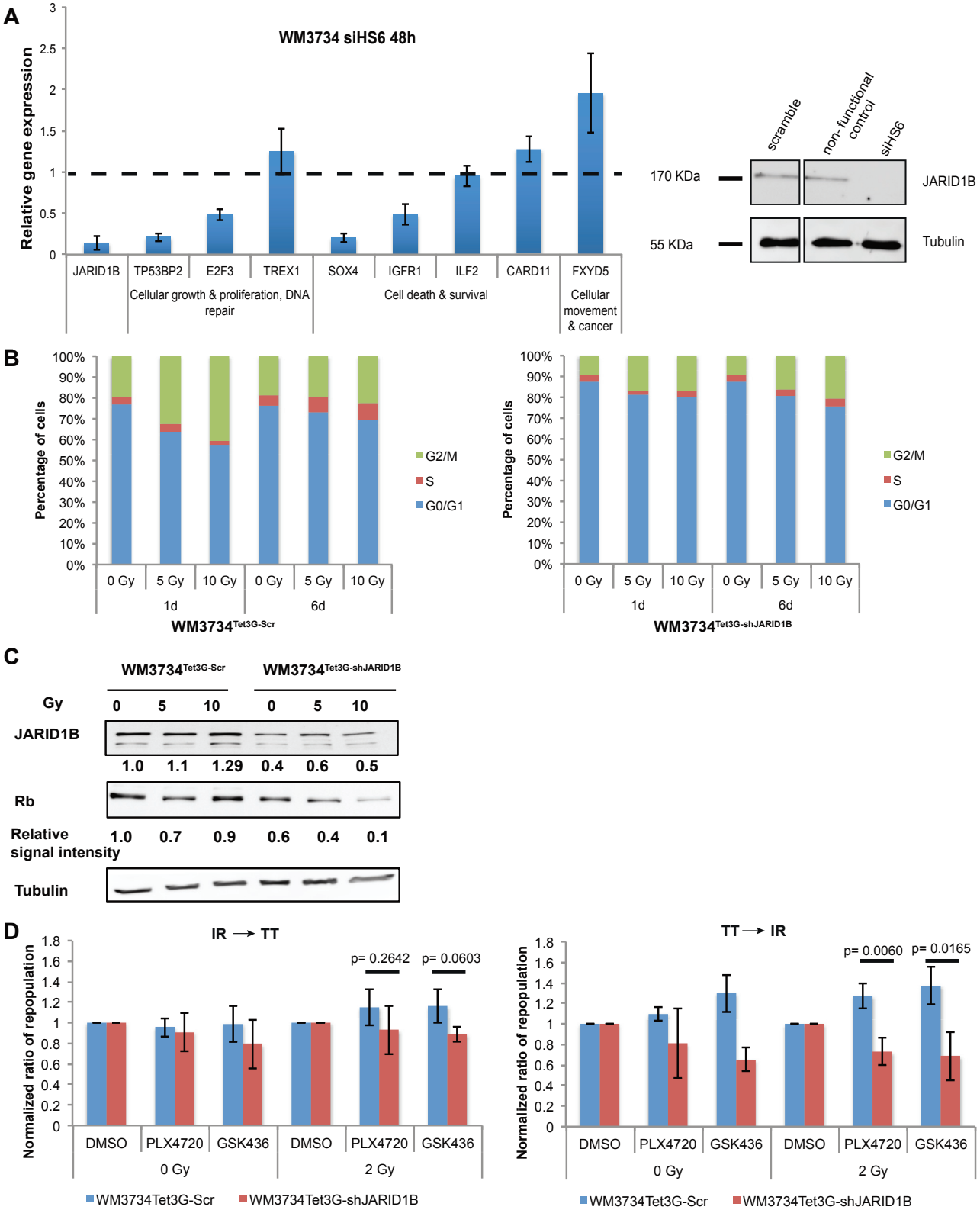

Fig. 6. **JARID1B-associated regulation of cell survival and cell cycle**. (A) *Left:* QPCR analysis of selected apoptosis, DNA repair and cell cycle regulatory genes after siRNA knockdown of JARID1B in WM3734 cells. JARID1B and genes' expression was compared to scramble control (set to 1 and indicated by dotted line). *Right:* Western blot confirmation of JARID1B knockdown. (B) Propidium iodide-based cell cycle analysis of $WM3734^{Tet3G-Scr}$ (*Left*) and $WM3734^{Tet3G\text{-}shJARID1B}$ (*Right*) cell lines 1 or 6 days after 0, 5 or 10 Gy irradiation. (C) Western blot analyses of JARID1B and pRb in $WM3734^{Tet3G-Scr}$ and $WM3734^{Tet3G\text{-}shJARID1B}$ melanoma cells at day 3 following either 0, 5 or 10 Gy radiation. (D) Quantification of crystal violet staining depicted as normalised ratios of cell repopulation to

were re-seeded in fresh medium at day 6 to examine their tumour repopulation properties. After 21 days, crystal violet staining indeed showed that cells surviving BRAFi or radiation can principally repopulate the cell culture and that the combination sequence TT → IR results in a significantly higher culture repopulation as compared with the opposite sequence (Fig. 3D, quantification shown in 3D right panel, p = 0.0212). Additional flow cytometry analysis of WM3734$^{JARID1Bprom-EGFP}$ cells at day 10 after treatment accordingly confirmed a higher increase of JARID1B^{high} cells in the TT → IR sequence (Fig. 3E).

Next, we analysed retrospectively collected clinical follow-up data of 65 stage IV melanoma patients with brain metastases for their intracranial responses after radiotherapy depending on the sequence of co-administered MAPK inhibition (MAPKi) (dabrafenib or vemurafenib as monotherapy or in combination with trametinib and cobimetinib) (for patient details, see Supplementary Table 2). Twenty-seven patients first received radiotherapy and then targeted therapy (IR → TT), i.e., their brain metastases were MAPKi-naïve at the time point of radiation. In contrast, the brain metastases of the other 38 patients had been first treated by MAPKi or developed under MAPKi and then were irradiated (TT → IR, with a median TT duration of 118 days). The intracranial responses were routinely staged by magnetic resonance imaging or computed tomography scans after an average time of 21.6 for 1st, 40.0 for 2nd, 60.2 for 3rd and 78.5 weeks for 4th staging after radiotherapy in the IR → TT group and 17.2, 36.5, 49.3 and 63.5 weeks in the TT → IR group. The intracranial tumour load as defined by the number of irradiated brain metastases was comparable between the two therapy groups (Supplementary Figure 3A). What is more, the different methods of radiation (fractionated stereotaxic, single stereotaxic, whole brain radiotherapy [WBRT] and WBRT + boost) were also comparable between the two therapy groups (Supplementary Fig. 3B and C). In fact, we observed that the brain metastases, which were treated with radiotherapy in the MAPKi-naïve situation, had a better and longer clinical response than metastases treated with upfront TT as indicated by a lower rate of intracranial progressive disease (Fig. 4A, B, and C; 16% versus 18% [p = 1.00], 16% versus 50% [p = 0.0157], 14% versus 53% [p = 0.0159] and 23% versus 60% [p = 0.1023] at 1st, 2nd, 3rd and 4th staging, respectively). Despite the limitations of such a non-controlled retrospective approach, this clinical 'real-world' observation considerably supports our *in vitro* and *in vivo* findings. However, it did not allow addressing the best time interval between radiotherapy and MAPKi, since therapy timing and staging time points were not standardised in the analysed patient cohort.

In sum, our preclinical and clinical results support the hypothesis that upfront treatment of melanoma cells with MAPKis could lead to a high enrichment for cross-resistant cell subpopulations followed by a high probability of tumour relapse.

3.4. *JARID1B expression favours the escape of melanoma cells from radiation*

To further explore the mechanistic basis for JARID1B-associated cell survival, JARID1B-dependent gene expression profiles were identified in publicly available human melanoma transcriptomes using the TCGA browser v0.9 software tool (see Materials and Methods for more details) [26,27]. Supplementary Table 3-sheet 1 shows the 669 genes that were identified by the TCGA browser to be co-regulated with JARID1B when the expression percentile was set to 10%. Subsequently, GO analysis was done for all the co-regulated genes (either significantly upregulated or downregulated if JARID1B is expressed) using the GSEA software [28,29]. The top 100 identified GO_pathways are shown in Supplementary Table 3-sheet 2. A subset of survival-relevant JARID1B-associated GO_pathways is shown in Fig. 5A. In addition, we aligned the 669 JARID1B co-regulated genes with Ingenuity™ signalling networks that are assigned either to cellular growth and proliferation, cellular movement and cancer, cell death and survival or DNA repair to further narrow down candidate genes that are both significantly co-regulated with JARID1B in melanoma and involved in cell survival (Fig. 5B and Supplementary Table 3- sheet 3). From those genes, CARD11, E2F3, IGF1R, TP53BP2, TREX1, ILF2, SOX4 and FXYD5 could be connected by Ingenuity™ in one signalling network and were picked for further confirmation (Fig. 5C).

Using JARID1B siRNA (clone HS6), we next confirmed the differential expression of the selected genes depending on short-term JARID1B knockdown (Fig. 6A). The way of expression regulation (upregulation or down-regulation depending on presence of JARID1B) matched with the co-expression levels seen before in our TCGA analysis (Supplementary Table 3). For functional analyses, we established a Tet3G-shJARID1B doxycycline-inducible system to ensure also long-term knockdown of JARID1B (Supplementary Figure 3D). Subsequent cell cycle analyses, which were performed up to 6 days after combined radiation and JARID1B knockdown, demonstrated a clear rescue from the G2/M arrest seen in respective scrambled controls (Fig. 6B) or before in naïve cells (Fig. 1). Additionally, we found a considerable decrease in

the respective DMSO control in WM3734$^{Tet3G-Scr}$ control and WM3734$^{Tet3G-shJARID1B}$ knockdown cells. The cells were treated as indicated in Fig. 3A, harvested on day 6, and the surviving cells were re-seeded (600 cells/well in 24-well plates). Cells were then allowed to repopulate for 3 additional weeks. *t*-Test shows a significant decrease in the repopulation ability in 2 Gy PLX4720 and GSK436 only in TT → IR sequence (p = 0.006 and 0.0165, respectively).

TT, targeted therapy; IR, radiation.

the expression of the cell cycle regulatory protein pRB following JARID1B knockdown further confirming the ability of JARID1B to stabilise pRb-mediated cell control knockdown matching JARID1B's previously described role in supporting cell cycle arrest via stabilisation of active pRB (Fig. 6C) [30]. The effect of JARID1B knockdown and pRB decrease on the protein level became particularly visible after cells were irradiated, i.e. when the surviving cell fraction normally is enriched for JARID1B.

Finally, we aimed to demonstrate that the repopulation ability of radiation-resistant melanoma cells is truly dependent on the presence of JARID1B. Thus, we repeated the repopulation experiment described in Fig. 3D now additionally using the Tet3G-shJARID1B doxycycline-inducible system (Fig. 6D). In brief, $WM3734^{Tet3G\text{-}shJARID1B}$ and $WM3734^{Tet3G-Scr}$ were sequentially co-treated as indicated in Fig. 3A, and surviving cells were re-seeded in fresh medium at day 6 to examine their tumour repopulation properties. Doxycycline induction was not stopped and was refreshed every 72 h. After 21 days, crystal violet staining was performed and quantified. We observed that $WM3734^{Tet3G\text{-}shJARID1B}$ cells showed decreased repopulation ability in both treatment sequences as compared with the respective scrambled controls, but, interestingly, this effect only became statistically significant in the TT → IR sequence, which also yielded before (see Fig. 3) in a higher enrichment for $JARID1B^{high}$ cells.

In sum, our preclinical experiments and retrospective clinical observations support the hypothesis that upfront treatment of melanoma cells with MAPKis could lead to a high enrichment for cross-resistant cell subpopulations followed by a high probability of tumour relapse.

4. Discussion

Despite the historic success of MAPK-targeted drugs (MAPKi) and immune checkpoint blockers in the therapy of advanced melanoma, most patients are still suffering from disease progression, particularly in critical anatomical locations such as the brain. Radiotherapy is a major treatment option in clinical routine that is commonly used to quickly control such critical organ metastases [1,31]. The combination of MAPKi plus radiation has been shown to effectively control melanoma cells in preclinical models and in clinical studies [8–10,32,33]. As a result, nowadays many patients receive (non-standardised) combinations of MAPKi plus radiotherapy. However, in light of the tremendous complexity of MAPKi-resistance that involves fundamental phenotypic switches in surviving cell subpopulations [2], it is currently not clear if such ill-characterised therapy combinations may even worsen disease progression and little is known on any potential cross-resistance mechanisms.

Our study demonstrates that melanoma cells which survived radiotherapy *in vitro* and *in vivo* are enriched for a cell subpopulation, which has been previously described by us and others to be slow-cycling, intrinsically multidrug-resistant and characterised by an elevated expression of the H3K4 demethylase JARID1B/KDM5B [16,18]. Certainly, we are aware that JARID1B-associated resistance only reflects a fractional part of the actual complexity of resistance in melanoma [16,18]. But since the radiation-induced enrichment of JARID1B seems to be a common phenomenon occurring across different tissue types including carcinomas like human oral cancer [34] and normal fibroblasts [25], we thought it might be worth investigating JARID1B's role as a universal cross-resistance marker, especially in models for the sequential combination of drugs and radiotherapy. Thus, we have set up a preclinical proof-of-principle platform to examine the influence of different therapy sequences (radiation and targeted therapy: IR → TT, TT → IR) on the degree of surviving melanoma cells using JARID1B as a surrogate marker for cross-resistance. Our results suggest that the level of $JARID1B^{high}$ cells is higher when melanomas are sequentially treated with upfront BRAFi followed by radiation as compared with upfront radiation followed by BRAFi. In congruence with previous findings on the elevated tumour repopulating capacity of $JARID1B^{high}$ melanoma cells [15], the *in vitro* treatment of melanoma cells with upfront MAPKi showed higher tumour repopulation than the reverse order. However, one limitation of our preclinical models is the use of a single radiation dose (10 Gy), which is not reflecting all different radiation regimens currently used in the clinics. Further investigations will address other clinically relevant settings, particularly fractionated low-dose radiation.

To analyse if the JARID1B enrichment after radiation also occurs in melanoma patients, we immunostained FFPE sections from 17 human melanoma brain metastases (n = 7 before and n = 10 after radiation treatment). Patients who were irradiated had a tendency of higher JARID1B expression (an example for a strong JARID1B enrichment is shown in Supplementary Figure 3E). However, this effect was not statistically significant across all the samples stained (Supplementary Figure 3E), probably because of the non-controlled and rather long time intervals between radiation and tissue collection (on average 6.3 months). Thus, comparable to the observations in our mouse xenografts, also relapsing human melanoma metastases may revert to a heterogeneous JARID1B expression pattern over time after initial radiation survival.

Owing to the lack of prospective clinical trial data, we performed a retrospective analysis of pooled unmatched real-life follow-up information (collaboratively collected within the German DeCOG network) to confirm our preclinical observations. An important drawback of this retrospective cohort was that patients were not stratified according to the time point of metastasis detection in the brain nor their overall tumour load making it difficult to

assess overall survival. As a result, local disease response to therapy was the only clinical response parameter that could be standardised for this study. Despite the limitations of such an approach, the comparison of the recorded staging results significantly supported the hypothesis that brain metastases, which received upfront radiotherapy followed by MAPKi therapy, have a better and more stable clinical response than MAPKi-pretreated metastases. In light of the present knowledge on the diversity and penetrance of MAPKi resistance mechanism in melanoma, this may be an expected result. However, to our knowledge, this is the first report that systematically examines melanoma responses to different sequences of radiotherapy and TT including underlying tumour-intrinsic cross-resistance mechanisms.

A first hint that our findings could also be true in a prospective setting comes from the recently published interim analysis of the COMBI-MB trial. Davies *et al.* have observed in this prospective phase 2 study that patients with asymptomatic melanoma brain metastases who received prior local therapy (whole brain radiotherapy, stereotactic radiosurgery, craniotomy) showed a better intracranial disease control rate, a better median intracranial duration of response and even a higher progression-free and overall survival than patients without prior local therapy (cohort B versus A) [35]. Certainly, this study was not designed to measure differences in sequential combination treatment of IR → TT versus TT → IR, and the effects seen could be just due to the additive effect of radiation plus systemic therapy irrespective of the therapy timing. Thus, further randomised trials are highly needed to address this unmet clinical need and improve daily therapeutic decision-making.

Regarding possible molecular mechanisms that mediate the multitherapy resistance of JARID1B^{high} melanoma cells, we found that JARID1B is co-expressed with a number of genes important for cellular movement (e.g., FXYD5), cell death and survival (e.g. CARD11, SOX4, IGF1R and ILF2) and cellular proliferation and DNA repair (e.g. TREX1, TP53BP2 and E2F3) in melanoma patients. This matches previous reports highlighting JARID1B's role as a key regulator of cellular homeostasis comprising not only survival and cell-cycle control but also in a broader context regulating cell fate and differentiation [15,36–38]. Moreover, Bayo *et al.* just recently showed that following radiation in lung cancer, the catalytic activity of JARID1B is required for complete and efficient repair of double-strand breaks. Also, knockdown of JARID1B phenocopies the effects of its pharmacological inhibition on DNA repair. Mechanistically, inhibition of JARID1B activity was demonstrated to result in defective recruitment of repair factors [19]. Since it is known that JARID1B is a histone demethylase and transcription factor that controls gene transcription on a genome-wide level [15,39–41], the factors selected here for proof-of-principle certainly represent only snippets of the entire picture. Nevertheless, the JARID1B-dependent regulation of cell survival and associated factors identified here seems to be evolutionarily conserved. Analysing mouse preimplantation embryos, Liu *et al.* have recently performed genome-wide analyses of H3K4me3 signatures in promoter regions via CHIP-Seq and identified gene signatures that are significantly co-regulated with JARID1B including also FXYD5, SOX4, IGF1R, ILF2, E2F3 and TREX1 [42]. Certainly, these results and especially the mechanism of JARID1B in cell proliferation and DNA repair in melanoma need further mechanistic evaluation in future studies.

In conclusion, we could establish a novel preclinical test platform to predict the outcome of different BRAFi-radiotherapy sequences in melanoma. The H3K4 demethylase JARID1B may represent a therapy-overarching resistance marker that could indicate the level of cross-resistance in melanoma. The evaluation of both our preclinical results and the retrospective analyses of patients' intracranial therapy responses supports a higher rate of tumour relapse when melanomas are treated with upfront MAPK inhibition as compared with upfront radiation. Further prospective studies with concomitant translational research programs are needed to further investigate the effects of radiotherapy combination sequences on patients' long-term responses.

Author contributions

B.S. and A.R. designed, planned and evaluated the experiments and wrote the manuscript. B.S., J.M., D.K. and A.H. performed the experiments. F.M., D.W., J.B., R.R., J.U., A.F., C.B., P.T., E.D., R.G., D.R.S., F.M., L.Z., E.L., M.S. and L.H. collected and provided the clinical data and the patients' tissues. D.S., V.J. and A.R. supervised the project. R.V., S.H. and J.K. helped with the statistical analysis. H.C., F.V., B.j.S. and M.S. contributed to the design and interpretation of the experiments. A.M., G.S. and T.G.P.G. provided the Tet-on inducible construct. All authors were involved in critical revision of the manuscript and approved the final submitted version.

Conflict of interest statement

None declared.

Acknowledgements

The authors thank A. Squire and A. Brenzel from the Imaging Centre Essen (IMCES) at the University Hospital Essen as well as T. Brockhoff, A. Paschen, I. Helfrich and S. Bauer for technical support; M. Benchallal for the assistance in *in vivo* work and M.

Herlyn for providing the WM3734 and WM9 melanoma cell lines. The research was supported in part by the Deutsche Forschungsgemeinschaft (DFG, German Research Foundation) grants RO3577/3-2 and GRK1739/2, the Hiege Foundation and the Monika-Kutzner Foundation. The laboratory of T: Grünewald is supported by grants from the German Cancer Aid (DKH-111886 and DKH-70112257).

Appendix A. Supplementary data

Supplementary data to this article can be found online at https://doi.org/10.1016/j.ejca.2018.12.024.

References

[1] Schadendorf D, Fisher DE, Garbe C, Gershenwald JE, Grob JJ, Halpern A, et al. Melanoma. Nat Rev Dis Primers 2015;1:15003.
[2] Roesch A. Tumor heterogeneity and plasticity as elusive drivers for resistance to MAPK pathway inhibition in melanoma. Oncogene 2015;34:2951–7.
[3] Parakh S, Park JJ, Mendis S, Rai R, Xu W, Lo S, et al. Efficacy of anti-PD-1 therapy in patients with melanoma brain metastases. Br J Canc 2017;116:1558–63.
[4] Goldman C, Tchack J, Robinson EM, Han SW, Moran U, Polsky D, et al. Outcomes in melanoma patients treated with BRAF/MEK-Directed therapy or immune checkpoint inhibition stratified by clinical trial versus standard of care. Oncology 2017;93:164–76.
[5] Warner AB, Postow MA. Combination controversies: checkpoint inhibition alone or in combination for the treatment of melanoma? Oncology (Williston Park) 2018;32:228–34.
[6] Pasquali S, Chiarion-Sileni V, Rossi CR, Mocellin S. Immune checkpoint inhibitors and targeted therapies for metastatic melanoma: a network meta-analysis. Cancer Treat Rev 2017;54:34–42.
[7] Westphal D, Glitza Oliva IC, Niessner H. Molecular insights into melanoma brain metastases. Cancer 2017;123:2163–75.
[8] Chowdhary M, Patel KR, Danish HH, Lawson DH, Khan MK. BRAF inhibitors and radiotherapy for melanoma brain metastases: potential advantages and disadvantages of combination therapy. Onco Targets Ther 2016;9:7149–59.
[9] Choong ES, Lo S, Drummond M, Fogarty GB, Menzies AM, Guminski A, et al. Survival of patients with melanoma brain metastasis treated with stereotactic radiosurgery and active systemic drug therapies. Eur J Cancer 2017;75:169–78.
[10] Trino E, Mantovani C, Badellino S, Ricardi U, Filippi AR. Radiosurgery/stereotactic radiotherapy in combination with immunotherapy and targeted agents for melanoma brain metastases. Expert Rev Anticancer Ther 2017;17:347–56.
[11] Hugo W, Shi H, Sun L, Piva M, Song C, Kong X, et al. Non-genomic and immune evolution of melanoma acquiring MAPKi resistance. Cell 2015;162:1271–85.
[12] Hong A, Moriceau G, Sun L, Lomeli S, Piva M, Damoiseaux R, et al. Exploiting drug addiction mechanisms to select against MAPKi-resistant melanoma. Cancer Discov 2018;8:74–93.
[13] Van Allen EM, Wagle N, Sucker A, Treacy DJ, Johannessen CM, Goetz EM, et al. The genetic landscape of clinical resistance to RAF inhibition in metastatic melanoma. Cancer Discov 2014;4:94–109.
[14] Gide TN, Wilmott JS, Scolyer RA, Long GV. Primary and acquired resistance to immune checkpoint inhibitors in metastatic melanoma. Clin Cancer Res 2018;24:1260–70.
[15] Roesch A, Fukunaga-Kalabis M, Schmidt EC, Zabierowski SE, Brafford PA, Vultur A, et al. A temporarily distinct subpopulation of slow-cycling melanoma cells is required for continuous tumor growth. Cell 2010;141:583–94.
[16] Roesch A, Vultur A, Bogeski I, Wang H, Zimmermann KM, Speicher D, et al. Overcoming intrinsic multidrug resistance in melanoma by blocking the mitochondrial respiratory chain of slow-cycling JARID1B(high) cells. Cancer Cell 2013;23:811–25.
[17] Tang B, Qi G, Tang F, Yuan S, Wang Z, Liang X, et al. JARID1B promotes metastasis and epithelial-mesenchymal transition via PTEN/AKT signaling in hepatocellular carcinoma cells. Oncotarget 2015;6:12723–39.
[18] Yuan P, Ito K, Perez-Lorenzo R, Del Guzzo C, Lee JH, Shen CH, et al. Phenformin enhances the therapeutic benefit of BRAF(V600E) inhibition in melanoma. Proc Natl Acad Sci U S A 2013;110:18226–31.
[19] Bayo J, Tran TA, Wang L, Pena-Llopis S, Das AK, Martinez ED. Jumonji inhibitors overcome radioresistance in cancer through changes in H3K4 methylation at double-strand breaks. Cell Rep 2018;25:1040–10450 e5.
[20] Matschke J, Riffkin H, Klein D, Handrick R, Ludemann L, Metzen E, et al. Targeted inhibition of glutamine-dependent glutathione metabolism overcomes death resistance induced by chronic cycling hypoxia. Antioxidants Redox Signal 2016;25:89–107.
[21] Iliakis G, Wang Y, Guan J, Wang H. DNA damage checkpoint control in cells exposed to ionizing radiation. Oncogene 2003;22:5834–47.
[22] Khanna KK, Lavin MF, Jackson SP, Mulhern TD. ATM, a central controller of cellular responses to DNA damage. Cell Death Differ 2001;8:1052–65.
[23] McKenna WG, Iliakis G, Weiss MC, Bernhard EJ, Muschel RJ. Increased G2 delay in radiation-resistant cells obtained by transformation of primary rat embryo cells with the oncogenes H-ras and v-myc. Radiat Res 1991;125:283–7.
[24] Tirosh I, Venteicher AS, Hebert C, Escalante LE, Patel AP, Yizhak K, et al. Single-cell RNA-seq supports a developmental hierarchy in human oligodendroglioma. Nature 2016;539:309–13.
[25] Chicas A, Kapoor A, Wang X, Aksoy O, Evertts AG, Zhang MQ, et al. H3K4 demethylation by Jarid1a and Jarid1b contributes to retinoblastoma-mediated gene silencing during cellular senescence. Proc Natl Acad Sci U S A 2012;109:8971–6.
[26] Cheng PF, Dummer R, Levesque MP. Data mining the cancer genome Atlas in the era of precision cancer medicine. Swiss Med Wkly 2015;145:w14183.
[27] Cancer Genome Atlas Research N, Weinstein JN, Collisson EA, Mills GB, Shaw KR, Ozenberger BA, et al. The cancer genome atlas pan-cancer analysis project. Nat Genet 2013;45:1113–20.
[28] Subramanian A, Tamayo P, Mootha VK, Mukherjee S, Ebert BL, Gillette MA, et al. Gene set enrichment analysis: a knowledge-based approach for interpreting genome-wide expression profiles. Proc Natl Acad Sci U S A 2005;102:15545–50.
[29] Mootha VK, Lindgren CM, Eriksson KF, Subramanian A, Sihag S, Lehar J, et al. PGC-1alpha-responsive genes involved in oxidative phosphorylation are coordinately downregulated in human diabetes. Nat Genet 2003;34:267–73.
[30] Roesch A, Becker B, Schneider-Brachert W, Hagen I, Landthaler M, Vogt T. Re-expression of the retinoblastoma-binding protein 2-homolog 1 reveals tumor-suppressive functions in highly metastatic melanoma cells. J Invest Dermatol 2006;126:1850–9.
[31] Zahnreich S, Mayer A, Loquai C, Grabbe S, Schmidberger H. Radiotherapy with BRAF inhibitor therapy for melanoma: progress and possibilities. Future Oncol 2016;12:95–106.
[32] Schick U, Kyula J, Barker H, Patel R, Zaidi S, Gregory C, et al. Trametinib radiosensitises RAS- and BRAF-mutated melanoma

by perturbing cell cycle and inducing senescence. Radiother Oncol 2015;117:364–75.
[33] Sambade MJ, Peters EC, Thomas NE, Kaufmann WK, Kimple RJ, Shields JM. Melanoma cells show a heterogeneous range of sensitivity to ionizing radiation and are radiosensitized by inhibition of B-RAF with PLX-4032. Radiother Oncol 2011; 98:394–9.
[34] Lin CS, Lin YC, Adebayo BO, Wu A, Chen JH, Peng YJ, et al. Silencing JARID1B suppresses oncogenicity, stemness and increases radiation sensitivity in human oral carcinoma. Cancer Lett 2015;368:36–45.
[35] Davies MA, Saiag P, Robert C, Grob JJ, Flaherty KT, Arance A, et al. Dabrafenib plus trametinib in patients with BRAFV600-mutant melanoma brain metastases (COMBI-MB): a multicentre, multicohort, open-label, phase 2 trial. Lancet Oncol 2017; 18:863–73.
[36] Facompre ND, Harmeyer KM, Sole X, Kabraji S, Belden Z, Sahu V, et al. JARID1B enables transit between distinct states of the stem-like cell population in oral cancers. Cancer Res 2016;76: 5538–49.
[37] Dey BK, Stalker L, Schnerch A, Bhatia M, Taylor-Papidimitriou J, Wynder C. The histone demethylase KDM5b/JARID1b plays a role in cell fate decisions by blocking terminal differentiation. Mol Cell Biol 2008;28:5312–27.
[38] Yamane K, Tateishi K, Klose RJ, Fang J, Fabrizio LA, Erdjument-Bromage H, et al. PLU-1 is an H3K4 demethylase involved in transcriptional repression and breast cancer cell proliferation. Mol Cell 2007;25:801–12.
[39] Klose RJ, Gardner KE, Liang G, Erdjument-Bromage H, Tempst P, Zhang Y. Demethylation of histone H3K36 and H3K9 by Rph1: a vestige of an H3K9 methylation system in Saccharomyces cerevisiae? Mol Cell Biol 2007;27:3951–61.
[40] Christensen J, Agger K, Cloos PA, Pasini D, Rose S, Sennels L, et al. RBP2 belongs to a family of demethylases, specific for tri- and dimethylated lysine 4 on histone 3. Cell 2007;128:1063–76.
[41] Iwase S, Lan F, Bayliss P, de la Torre-Ubieta L, Huarte M, Qi HH, et al. The X-linked mental retardation gene SMCX/JARID1C defines a family of histone H3 lysine 4 demethylases. Cell 2007;128:1077–88.
[42] Liu X, Wang C, Liu W, Li J, Li C, Kou X, et al. Distinct features of H3K4me3 and H3K27me3 chromatin domains in preimplantation embryos. Nature 2016;537:558–62.
[43] Forsberg K, Valyi-Nagy I, Heldin CH, Herlyn M, Westermark B. Platelet-derived growth factor (PDGF) in oncogenesis: development of a vascular connective tissue stroma in xenotransplanted human melanoma producing PDGF-BB. Proc Natl Acad Sci U S A 1993;90:393–7.
[44] Satyamoorthy K, Soballe PW, Soans F, Herlyn M. Adenovirus infection enhances killing of melanoma cells by a mitotoxin. Cancer Res 1997;57:1873–6.
[45] Wiederschain D, Wee S, Chen L, Loo A, Yang G, Huang A, et al. Single-vector inducible lentiviral RNAi system for oncology target validation. Cell Cycle 2009;8:498–504.
[46] Vultur A, Herlyn M. Cracking the system: melanoma complexity demands new therapeutic approaches. Pigment Cell Melanoma Res 2009;22:4–5.